FISEVIER

Contents lists available at ScienceDirect

# Sustainable Energy Technologies and Assessments

journal homepage: www.elsevier.com/locate/seta



# Outdoor behaviour of organic photovoltaics on a greenhouse roof

Esther Magadley<sup>a,\*</sup>, Meir Teitel<sup>b</sup>, Maayan Friman Peretz<sup>b,c</sup>, Murat Kacira<sup>d</sup>, Ibrahim Yehia<sup>a</sup>

- <sup>a</sup> Triangle Research and Development Center, P.O. Box 2167, Kfar-Qari 30075, Israel
- b Institute of Agricultural Engineering, Agricultural Research Organization, The Volcani Center, HaMaccabim Road 68, P.O. Box 15159, Rishon LeZion 7528809, Israel
- <sup>c</sup> Department of Mechanical Engineering, Ben-Gurion University of the Negev, P.O. Box 653, Beer-Sheva 81405, Israel
- d Department of Biosystems Engineering, The University of Arizona, Tucson, AZ 85721, USA

#### ARTICLE INFO

Keywords:
Organic photovoltaics
Greenhouse integrated photovoltaics
Outdoor data
Incident irradiance and temperature
dependence
Overnight recovery

#### ABSTRACT

This study presents a detailed analysis of the outdoor behaviour of organic photovoltaic (OPV) panels on a polytunnel type greenhouse roof in a Mediterranean climate, looking at the effects of environmental variables and panel orientations on the electrical behaviour and degradation of the panels, thus providing crucial outdoor testing results of greenhouse integrated OPVs in this climatic region.

The OPV panel placed at the polytunnel ridge of the roof yielded highest outputs, efficiencies and fill factors during the measurement period. However, the use of panels on the East and West sides of the greenhouse roof, could reduce midday output peaks and therefore provide a more balanced power supply throughout the day.

The diurnal variation in OPV behaviour was influenced by simultaneous effects of changing irradiance and temperature. It was found that although output was higher, the OPVs showed dips in fill factor and efficiency at times with high incident irradiance. This was assumed to be due to a reversible degradation phenomenon under high direct irradiance conditions, which led to higher performance during morning hours compared to the afternoon and was followed by a recovery overnight and to some extent in shaded conditions.

#### Introduction

Combining commercial agriculture and photovoltaic electricity production on the same area of land (agrivoltaics) is an increasingly researched area as a strategy to increase overall land productivity in an increasingly densely populated world [1-4]. Different methods of integrating photovoltaics (PV) into greenhouses have previously been studied, such as partially covering the greenhouse roof using silicon PV and therefore partially shading the crops below [1,4-7]. Semi-transparent organic photovoltaics (OPV) have shown great potential for different building integrated PV applications [8] and could also be better suited as part of a greenhouse cover than opaque silicon PVs. OPVs have the following advantages: they are lightweight, flexible and importantly, their absorption spectra can be tuned to mainly absorb light not needed for crop growth allowing the remaining light to reach the plants [9]. OPVs also have a low carbon footprint, are easily recycled/decommissioned and they are predicted to have much lower production costs than silicon PVs when mass produced in the near future [10-12]. In addition, the polyethylene substrate material used in OPVs is similar to the covers of polyethylene-covered greenhouses, making the integration of OPVs into greenhouse covers an interesting possibility.

Emmott et al. [9] carried out a techno-economic analysis of an organic photovoltaic greenhouse, by evaluating the impact on crop growth of different OPV materials on a greenhouse and the efficiency and spectral transparency of a variety of semi-conducting polymer materials. Their economic analysis suggested there could be a huge potential for OPV greenhouses if the predicted OPV cost reductions happen. They also concluded that although semi-transparent OPV devices struggle to perform better than opaque crystalline silicon with partial coverage, OPV devices using PMDPP3T and PCDTBT materials showed better performance compared to opaque, flexible thin-film modules such as CIGS (Copper-Indium-Gallium-Selenide). Benatto et al. [13] carried out two-year outdoor stability tests of OPVs with two different device architectures inside a glass greenhouse in the Netherlands and found that module lifetime was improved slightly, by having them inside the greenhouse, being protected from the weather. Various simulation models have been developed, to find the optimum OPV coverage in terms of output and crop quality [14,15] which was found to be between 24 and 30% OPV roof coverage. Peretz et al [16] examined the radiometric and thermal properties of an OPV module to assess its suitability as a greenhouse cover and concluded that OPVs could potentially be used to shade greenhouses to reduce excess solar energy and to produce electricity. However, if the application of OPVs

E-mail address: esther.magadley@trd-center.org (E. Magadley).

<sup>\*</sup> Corresponding author.

Nomenclature		PV	photovoltaics	
		RH	relative humidity (%)	
$A_c$	collector active area (m <sup>2</sup> )	Si-PV	silicon photovoltaics	
CIGS	Copper-Indium-Gallium-Selenide	$T_a$	outdoor ambient temperature (°C)	
E	incident irradiance (W/m²)	$T_{\rm m}$	module temperature (°C)	
FF	fill factor	$V_{mp}$	voltage at maximum power point (V)	
$I_{mp}$	current at maximum power point (A)	$V_{oc}$	open circuit voltage (V)	
$I_{sc}$	short circuit current (A)	$\Delta T$	ambient - module temperature difference (°C)	
I-V	current-voltage	θ	solar incidence angle (°)	
OPV	organic photovoltaics	η	efficiency (%)	
$P_{max}$	maximum power point (W)			

on greenhouse roofs is to become widespread, in addition to investigating the effect on the crops in the greenhouse, it is vital to understand the electrical behaviour of the OPV panels in a greenhouse application by carrying out outdoor studies. Hirata et al. [17] investigated the output of OPVs in different orientations on a curved roof using a  $40\times60$  cm greenhouse model outputs varied depending on the location and orientation of the panels. However due to the small size of the model the curvature was more pronounced than on a full-sized greenhouse.

Other OPV outdoor lifetime studies were carried out in different parts of the World, such as Krebs et al. [18] in their round robin study and others listed by Zhang et al. [19] in several countries including Denmark, UK, Holland, Germany, USA, Australia, India and Israel. Bristow & Kettle [20] presented the outdoor dependence of temperature and irradiance on the performance of inverted organic photovoltaic modules in a cooler Welsh climate during summer and winter seasons, Emmott et al. [21] carried out a field-trial of OPV technology installed on corrugated steel roofs at two sites in a rural village in Southern Rwanda, exposed to very high levels of insolation (especially UV), high temperatures and heavy rainfall. This led to a 5-6 times reduction of module lifetimes compared to control modules kept both in the dark and outdoors in Roskilde, Denmark. They showed that degradation was mainly due to extensive delamination caused by failure of the non-UV stable encapsulation. Stoichkov et al. [22] studied the outdoor performance of organic building-integrated photovoltaics laminated to the cladding of a building prototype and showed the significance of module orientation for energy yield across diurnal and seasonal changes. They found that the top-facing module had the highest energy yield overall and that west facing modules however could significantly contribute to power generation during peak power periods in a building application. Hartner et al. [23] also found that angle combinations that maximize the diurnal and annual output of a PV system are economically interesting.

This paper presents the outdoor performance of OPVs installed at

three different orientations on the roof of a polytunnel under a Mediterranean climate, throughout a period of 12 weeks (from 18th October 2018 to 13th January 2019). The autumn/winter measurement period of this study included different kinds of weather conditions, within a short time span. This enabled the investigation of how different weather conditions affect the performance of OPV panels on a greenhouse roof. The effect of temperature and irradiance on the OPV panels' behaviour in terms of power output, open circuit voltage ( $V_{\rm oc}$ ), short circuit current ( $I_{\rm sc}$ ), efficiency ( $\eta$ ) and fill factor (FF) is presented, in particular the effect of diffuse and direct irradiance and solar incidence angles. In addition, the degradation of the OPV panels is discussed.

#### Materials & methods

To study the feasibility of using OPV on a tunnel roof, 2 tunnel greenhouses were built, both in North-South orientation, in the town of Kfar Qara, Israel (latitude and longitude 32.5055 °N, 35.0543 °E): one with OPVs mounted on the roof and another served as control greenhouse without OPVs. The polytunnels, were made of a metal frame covered with polyethylene film. Fig. 1 shows the OPV panel arrangement on the tunnel roof.

The OPV devices were PBTZT-stat-BDTT-8 based fully solution coated, semi-transparent and flexible organic photovoltaic modules. The device structure, similar to the devices used by BElectric in their Solar Trees at the Universal Exhibition Milan 2015, is described in detail by Berny et al. [24]. The panels were manufactured by Opvius (Germany) had a thickness of 0.6 mm module and dimensions  $800\times1000$  mm with an active area of 655  $\times$  855 mm (Fig. 2). Each panel consisted of 4 serially connected devices, with a rated cell efficiency at STC of 3.3%, nominal power of 14  $W_p$  and the following rated temperature coefficients: temperature coefficient of  $V_{\rm oc}=-0.19\%/K$ , temperature coefficient of  $I_{\rm sc}=+0.08\%/K$  and temperature coefficient of  $P_{\rm max}=+0.02\%/K$  (Opvius data sheet).





Fig. 1. OPV panel arrangement on the tunnel roof. Photos were taken from outside (left) and inside the tunnel (right) respectively.

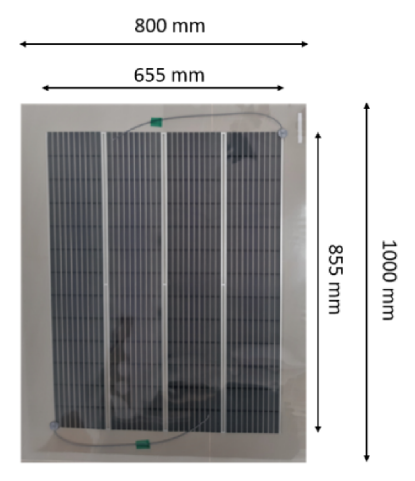


Fig. 2. Dimensions of the OPV panels.

The OPV panels were connected to form strips of several OPVs of 1 m width and about 6.4 m length. They were arranged across the arch of the greenhouse roof with 1 m spaces in between adjacent strips, as shown in Figure 1. In total, there were 9 strips consisting of 8 individual OPV panels and one strip with 10 panels on the Northern end of the roof. The OPV strips were fixed to the roof sheeting using adhesive tape (ETFE-foil coated with polysiloxane adhesive, CMC, Germany) along the edges of the strips.

The 10 panel strip (A) was used to monitor the electrical behaviour of the panels across the curve of the roof. Although all 10 panels in row A1 on the greenhouse roof were initially monitored, 7 panels out of ten in the A1-10 strip stopped working within only a few weeks of installation. This paper discusses the electrical behaviour of the remaining 3 working OPV panels A2, A6 and A9 (Fig. 3): A2 @ 21° tilt facing West, A6 @ 11° tilt facing East on the top and A9 @ 27° tilt facing East on the greenhouse roof. Panel A6, although on the top part of the roof, was not fully on a horizontal plane, resulting in the behaviour of A6 being closer to that of A9, as they were both facing East. In addition, a polycrystalline silicon PV (Si-PV) panel from Bluesun Solar, China with the following specifications was installed on a frame at a tilt angle of 30° facing South at a height of 2.5 m above the ground, unaffected by shading: Model type: BSM-045P, Solar cell type: Poly 156 × 156 cell, Panel size:  $660 \times 550 \times 30$  mm,  $P_{max} = 45$  W,  $V_{mp} = 17.6$  V,  $I_{mp} = 2.56A$ ,  $V_{oc} = 21.9 V$ ,  $I_{sc} = 2.85A$  @STC.

The data collection setup followed the ISOS-O-2 outdoor measurement protocol [25], however the OPV panels were on a tunnel roof, rather than standard frames at 0 or 30° tilt, to simulate operation under real agricultural conditions. The data collected for each panel included

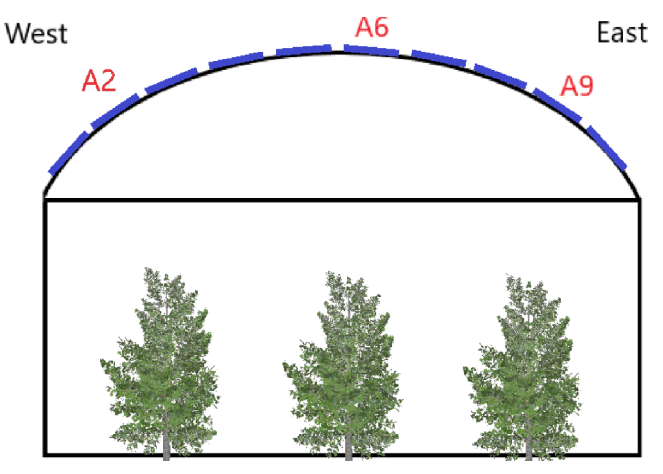


Fig. 3. OPV panels across the roof in row A.

current-voltage (I-V) curves as well as the module incident irradiance (E) and module temperature ( $T_m$ ), which were measured at 10 min intervals during daylight hours (panels were held at open circuit between measurements). In addition, outdoor ambient temperature ( $T_a$ ) and relative humidity (RH) were recorded. From the I-V curves, maximum power points ( $P_{max}$ ) were found and fill factor (FF) and the panel efficiency ( $\eta$ ) were calculated for each reading using the following equations:

Efficiency (%), 
$$\eta = P_{max}/(E * A_c) * 100$$
 (1)

Fill factor, 
$$FF = P_{max}/(V_{oc} * I_{sc})$$
 (2)

where  $P_{max}=$  Maximum power point (W), E= Incident irradiance (W/m<sup>2</sup>),  $A_c=$  collector active area (m<sup>2</sup>),  $I_{sc}=$  short circuit current (A) and  $V_{oc}=$  open circuit voltage (V)

Three *EKO ML-02 pyranometers* (EKO Instruments, Netherlands) were used to measure incident irradiance (E) for the 3 panels. T type thermocouples were attached to the underside of the OPV panels to record the OPV module temperatures (T<sub>m</sub>). A *Keithley 2460 Sourcemeter* (Tektronix, USA) was used to measure the I-V curves and a *Keithley 2701 digital multimeter* (Tektronix, USA) to take irradiance and module temperature readings, as well as switching between channels for the OPV panels. A LabView (National Instruments, USA) program was developed to control both devices to take readings every 10 min during daylight hours and to record the data in an Excel spreadsheet. A *Teltonika* (Vilnius, Lithuania) *TZ-BT04 BLE temperature and relative humidity data logger* recorded outdoor ambient temperature and relative humidity.

To measure the effect of different solar incidence angles on the electrical behaviour of the OPV panels, a smaller OPV sample (dimensions:  $190\times870$  mm, active area:  $160\times850$  mm) of the same type and manufacturer of OPV was used and tested on two days 20 and 24.03.2019 as follows: The tilt angle with the sun at  $90^\circ$  to the OPV panel (normal to the panel) was found and then changed with increments of  $10^\circ$  from  $0^\circ$  to  $60^\circ$  angles of incidence. For each angle increment, the incident irradiance was recorded using an EKO ML-02 pyranometer connected to a handheld multimeter as well as the I-V curve using the Keithley 2460 Sourcemeter. From this, the  $P_{\rm max}$ , FF and efficiency values were calculated.

#### Results and discussion

Fig. 4 summarises the measurements of panels A2, A6, A9 and the reference Si-PV panel from 18th October 2018 to the 13th January 2019. The measurement period started off with mainly sunny days with high irradiance and temperatures and no rain. Irradiance and ambient temperature figures decreased from October 2018 to January 2019 and the number of overcast and rainy days increased. Incident irradiance E decreased slightly for all panels over the measurement period, with the Si-PV at tilt 30° south receiving the highest overall irradiance (Fig. 4a). Module temperatures decreased in a similar way for all panels and the Si-PV overall had marginally higher temperatures (Fig. 4b). (The temperature sensor of panel A6 failed from the 1.12.2018 to the 17.12.2018.) The OPV panels maximum power outputs (Pmax) decreased slightly over the measurement period, whereas the Si-PV outputs remained relatively constant (Fig. 4c). Efficiency and Fill factor (FF) values decreased very slightly over the measurement time for the OPV panels (Fig. 4d&g) and slightly increased for the Si-PV with lower ambient temperatures due to the negative temperature coefficients of the later. Open circuit voltage figures showed a very slight decrease due to the increased number of overcast days in the second half of the measurement period (Fig. 4e). The source-meter device used for the measurements could only carry out a current voltage sweep up to 20 V for the higher current of the Si-PV and therefore could not record the actual Voc for the Si-PV at all times. Short circuit current (Isc) values show a more significant reduction following the incident irradiance

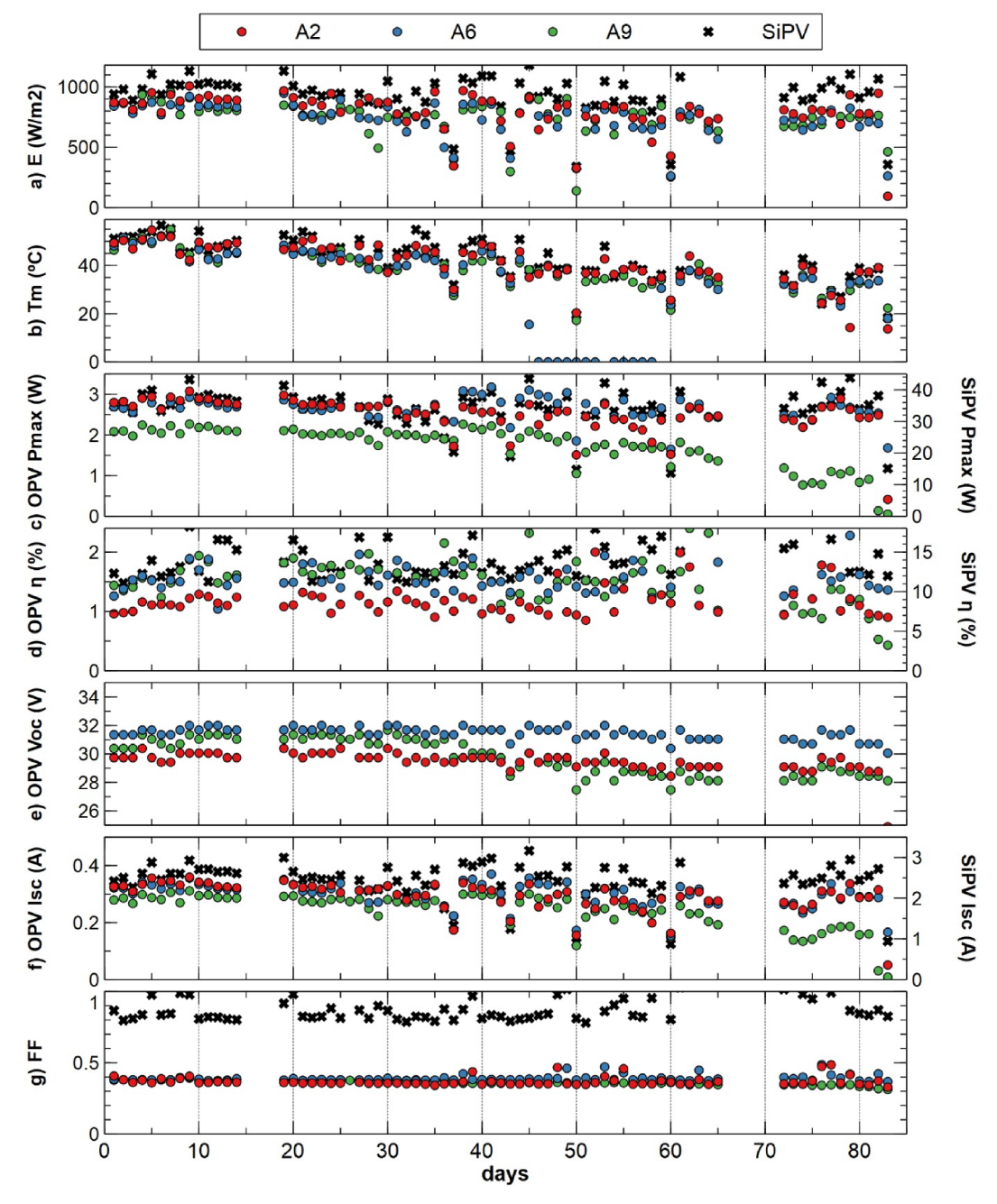


Fig. 4. Daily maximum value of E (a),  $T_m$  (b),  $P_{max}$  (c),  $\eta$  (d),  $V_{oc}$  (e),  $I_{sc}$  (f), FF (g) for OPV panels A2, A6, A9 and Si-PV from 18.10.2018 to 13.1.2019.

values (Fig. 4f).

Panel A9 behaved differently when compared to the other OPVs, with lower efficiency and power output. From the end of December onwards, a dramatic reduction in power output, current and voltage was recorded, which was due to the physical and consequent electrical degradation. As expected, Table 1 shows that the reference Si-PV panel by far outperformed the OPV panels throughout the measurement period due to its much higher efficiencies compared to the OPVs. The generally low efficiencies of the OPV panels measured in this study were mainly attributed to the fact that the measurements reported here were taken after the initial 'burn in' period of the panels and therefore represent lower outputs than the initial 3.3% efficiency rating under STC from the manufacturer. Other factors such as varying temperature, irradiance levels and angles of incidence throughout the day, due to the location of the panels on the tunnel roof, also led to lower outputs than expected.

Although the three OPV panels on the greenhouse roof had roughly the same accumulated incident solar energy of around 121 kWh throughout the measurement period, their average efficiencies and total outputs varied (Table 1). OPV A9 had the lowest performance values

**Table 1**Output and average efficiencies and fill factors for panels A2, A6, A9 and the reference Si-PV at 30° south from 18.10.2018 to 13.1.2019.

	OPV A2	OPV A6	OPV A9	Si-PV
Overall output (Wh)	839.49	997.46	711.42	10166.97
Output per m <sup>2</sup> (Wh/m <sup>2</sup> )	1519.44	1805.35	1287.64	28008.18
Daily average η (%)	0.69	0.82	0.58	10.50
Average morning (6:00-10:30) η (%)	0.86	1.10	0.72	11.17
Average midday (10:40-13:30) η (%)	0.72	0.86	0.61	10.50
Average afternoon (13:40-17:30) η (%)	0.56	0.80	0.89	8.15
Daily average FF	0.32	0.33	0.29	0.71

due to its dramatic degradation at the end of the measurement period. Yano et al. [5] studied the use of amorphous silicon PV panels on a greenhouse roof in similar orientation as the one in this study and found that the panels near the top of the greenhouse roof with lower tilt angles generated more electrical energy. Hirata et al. [17] measured accumulated output ratios of curved panels on the curve of a greenhouse model and found that average accumulated output ratios of curved panels in East, top and West locations were 0.90, 1.01 and 0.72 respectively in relation to the output of a reference OPV module on a horizontal surface for panels with cells along the greenhouse (North to South). A similar outcome was found for OPVs in this study: Panel A6 on the top of the roof had the highest yield, average efficiency and average fill factor of the three OPV panels (A2, A6 and A9), indicating this might therefore be the best location for the OPVs to achieve maximum electrical output. However, as other studies showed [22,23], the inclusion of panels in other orientations can provide a diurnally and annually more distributed energy supply to the greenhouse, therefore balancing energy supply and demand.

Taking the average output of the 3 panels monitored over the measurement period, and assuming 82 OPV panels (totalling 45.9 m<sup>2</sup> active area) were used, covering 26% the greenhouse roof, the OPV system output would be about 70 kWh during the measurement period of 88 days. To match this output, 7-8 polycrystalline silicon panels of the type used in this study (around 2.5 m<sup>2</sup>) at 30° tilt angle facing south would be required. Annual producible electricity of the 82 OPV panels would be about 500 kWh, based on the performance data collected and average values of annual irradiance [26]. This is equivalent to 3 kWh/ m<sup>2</sup> of tunnel area per year, slightly lower than the estimate of 4.9 kWh/ m<sup>2</sup> from Okada et al.'s simulation [14]. Campiotti et al. [27] report the annual electricity demand of a Mediterranean greenhouse at between 2 and 9 kWh/m<sup>2</sup>. The output of this OPV system would therefore cover the lower estimate of electricity demand. However, since the OPV cover in this study has been shown to be an effective shading device [16], the electricity demand of the greenhouse would be slightly reduced due to the consequently lower cooling demands in the summer. Therefore, this OPV cover is expected to be able to cover a large part of the electricity demand of a typical Mediterranean greenhouse.

Considering the average efficiencies for the OPV panels at different times of the day in Table 1, the data seems to indicate that efficiencies were highest at times when the OPV panels received mainly diffuse radiation (such as in the morning for panel A2 and in the afternoon for panel A9) and not during hours with highest direct irradiance and panel temperatures. To understand this behaviour in more detail, the effects of temperature and irradiance are investigated in the following sections.

### Effect of temperature on OPV panels' behaviour

Fig. 5 shows the diurnal temperature differences from ambient temperature ( $\Delta T$ ) of the OPV panels (A2, A6 and A9) for a sunny (17th November 2018) and a cloudy day (23rd November 2018).  $\Delta T$  is defined as:

$$\Delta T = T_m - T_a \tag{3}$$

where  $T_m$  = panel temperature (°C) and  $T_a$  = ambient outdoor temperature (°C).

The curves in Fig. 5 have a similar shape to the incident irradiance curves for the three panels. This is further shown in Fig. 6 which shows that  $\Delta T$  increased with incident irradiance in an approximately linear manner both on the sunny and the overcast days. On the overcast day, all three OPV panels behaved in a similar way, due to them receiving similar mainly diffuse radiation. On the sunny day however, differences can be seen in terms of panel temperature behaviour, due to the fact

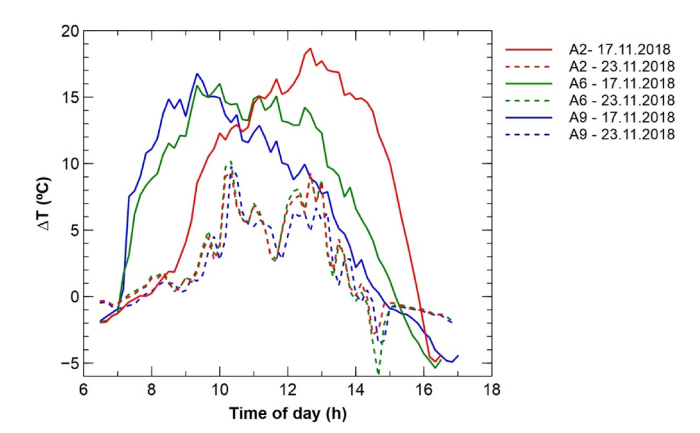


Fig. 5. Diurnal change of temperature difference  $(T_m-T_a)$  (°C), for the 17.11.2018 (solid lines) and 23.11.2018 (dashed lines).

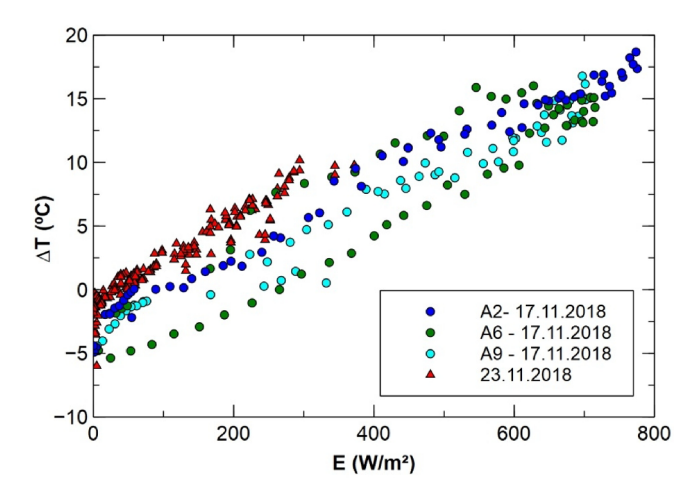


Fig. 6. Temperature difference  $(T_m-T_a)$  (°C) vs. incident irradiance  $(W/m^2)$ .

that the panels' incident direct irradiance peaked at different times of the day for each panel due to their locations on the roof. In addition to irradiance, wind speed, relative humidity and ambient temperature would also have influenced module temperature. The negative  $\Delta T$  values at low irradiance in Fig. 6 and late afternoon in Fig. 5 are assumed to be due to radiative cooling of the modules.

Fig. 7 shows the irradiance, outdoor ambient temperature and relative humidity for the two selected days. As well as irradiance, mean daily outdoor ambient temperature, on the sunny day, was higher (around  $5.5~^{\circ}$ C) and mean daily outdoor relative humidity was 18.5% lower.

Due to the fact that module temperatures increased with irradiance, and in order to understand the effect of temperature alone on the OPV performance, the data was filtered for two different irradiance ranges:  $500~\pm~20~\text{W/m}^2$  and  $800~\pm~20~\text{W/m}^2$  for panel A6 at the top of the greenhouse, using a short time frame (18–28.10.2018 only), so that the effect of ambient conditions and degradation would not be significant in this shorter timeframe. The data was also divided into AM and PM data. The module temperatures during that period, for both data sets, ranged between 25 and 55 °C.

Fig. 8 shows that  $P_{\rm max}$ ,  $V_{\rm oc}$  and  $I_{\rm sc}$  values were higher and efficiency and fill factor values were lower for the 800 W/m<sup>2</sup> data set compared to the 500 W/m<sup>2</sup> data set. The 500 W/m<sup>2</sup> data values were generally more scattered presumably since they included incident irradiance with

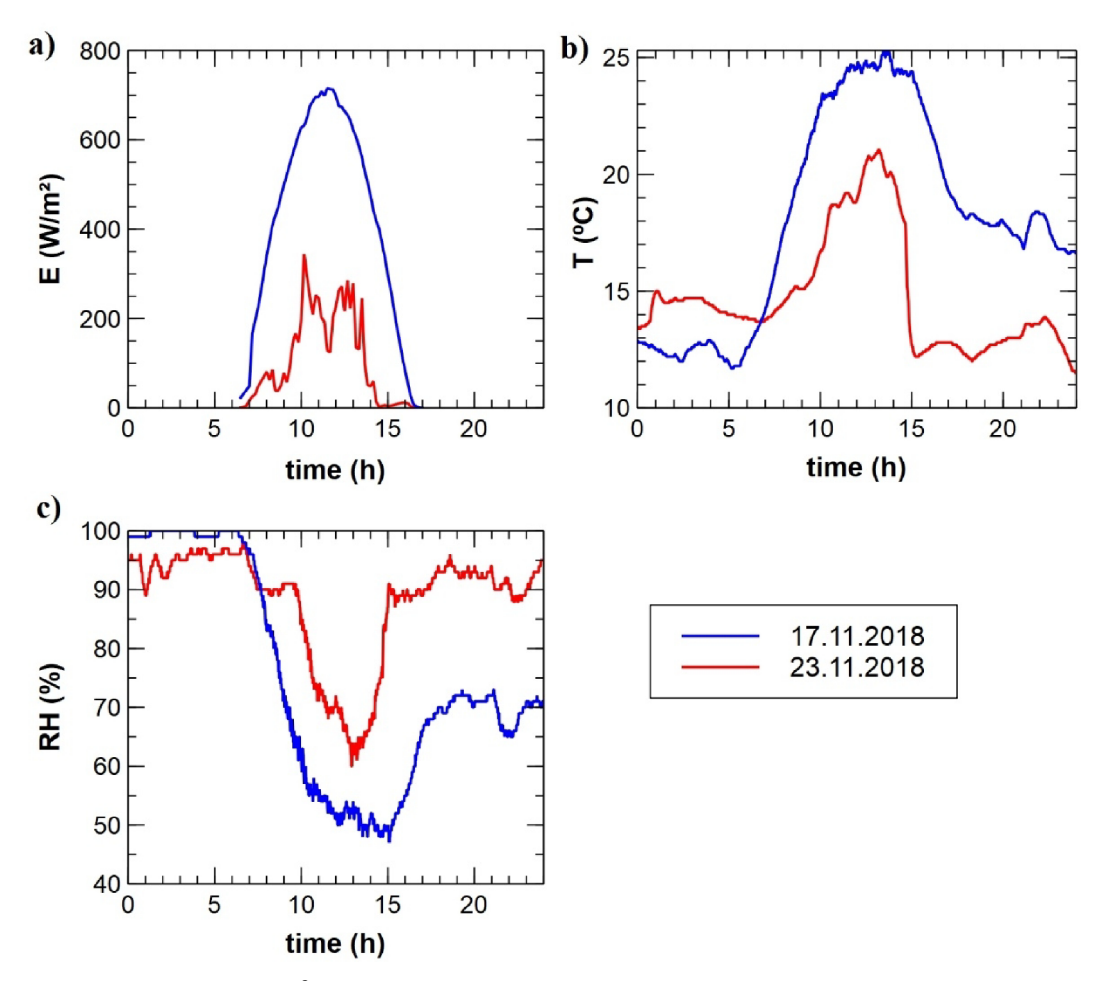


Fig. 7. a) Irradiance on the horizontal plane  $(W/m^2)$ , b) outdoor ambient temperature (°C) and c) relative humidity (%) for the 17.11.2018 (blue line) and the 23.11.2018 (red line).

different spectral characteristics (due to varying solar incidence angles and times of day). In addition, mismeasurements when light levels changed during measurement periods may also have influenced the readings. Differences in performances of the OPV panels can be seen between the AM and PM data sets, indicating a decline of performance throughout the day, followed by an overnight recovery of the active material and therefore a higher performance in the morning hours. This phenomenon can especially be seen for  $I_{\rm sc},\,P_{\rm max}$  and  $\eta$  values and is mainly apparent for the 500 W/m² data. FF values however were higher for the PM data. The high irradiance data of 800 W/m² data is assumed to be the time of the decrease in efficiency and therefore shows a less pronounced difference between AM and PM data.

Manufacturer's specifications detail positive temperature coefficients of  $I_{sc}=+0.08\%/K$  and  $P_{max}=+0.02\%/K$ . This slight increase in  $P_{max},\ I_{sc}$  and  $\eta$  with increased module temperature is observed between 40 and 55 °C for the 800 W/m² and between 35 and 45 °C for the 500 W/m² in the afternoon measurements, concurring with other studies in the literature reporting positive temperature coefficients for OPV devices [18,20,28].

However, the morning data shows a slight decrease in  $\eta$  with increased module temperature at both irradiance levels (Fig. 8), suggesting a negative temperature coefficient of the panels at this time of day. This trend could be related to the suggested overnight recovery of the panels, where  $\eta$  is higher first thing in the morning and reduces

throughout the morning which coincides with an ambient temperature rise.

 $V_{\rm oc}$  values decreased linearly with increase in temperature at the temperature range 40–55 °C similar to the trend reported by Elumalai and Uddin [29] and Krebs et al. [18], again tying in with the manufacturer's specifications temperature coefficient of  $V_{\rm oc}=-0.19\%/K$ . However, the voltage decrease was less significant compared to the current increase with temperature and therefore had less of an effect on the overall power output. Fill factor values stayed relatively constant with increasing temperatures.

## Effect of irradiance on OPV panels' behaviour

To investigate the effect of irradiance on panels placed on a curved greenhouse roof, the following factors were considered: 1) intensity, 2) direct and diffuse radiation and 3) the solar incidence angle.

As Fig. 8 showed,  $P_{max}$ ,  $V_{oc}$  and  $I_{sc}$  values were higher and  $\eta$  and FF values were lower for the higher compared to the lower irradiance data set, particularly at the low range of panel temperatures. The graphs in Fig. 9 show the effect of increasing irradiance on the various electrical parameters of the three OPV panels and the Si PV panel. Module temperatures rose with incident irradiance for all panels (Fig. 9a) and therefore peaked at the times they receive the highest direct radiation (A9 in the morning, A6 at midday and A2 in the afternoon). The overall

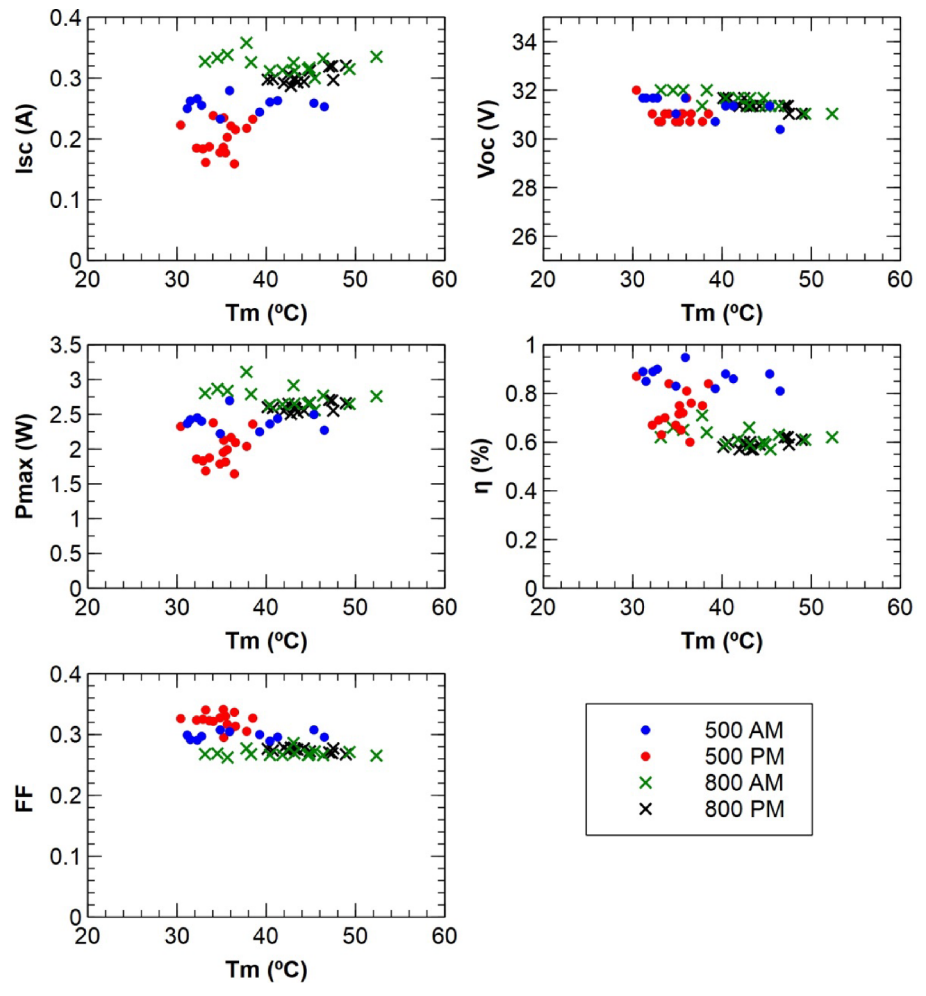


Fig. 8. Effect of temperature on OPV characteristics (panel A6) for irradiances 500 W/m<sup>2</sup> and 800 W/m<sup>2</sup>.

OPV and Si-PV panel temperature ranges were similar. The change in  $P_{\rm max}$  with irradiance is shown in Fig. 9b, showing a general rise in  $P_{\rm max}$  with irradiance, which is linear for the Si-PV in line with  $I_{\rm sc}.$  However, for the OPV panels, the rise is not linear since  $P_{\rm max}$  is affected by current, voltage and fill factor. Short circuit current ( $I_{\rm sc}$ ) of the OPV modules increased with irradiance as seen in Fig. 9e similar to that of Krebs et al. [18]. Open circuit voltage rose logarithmically with illumination intensity in agreement with Elumalai and Uddin [29] as can be seen in Fig. 9d reaching limiting values at around 200 W/m² irradiance. The function best fitting the data points is  $V_{\rm oc}=30(1-\exp{(-E/50)}.~I_{\rm sc}$  for the Si PV rose linearly with irradiance.

OPV peak efficiency (Fig. 9c) and fill factor (Fig. 9f) values were observed at very low irradiance values (around  $100~\text{W/m}^2$ ) and declined with increasing irradiance, a phenomenon also observed in De Amorim Soares et al. [30] lifetime study of different photoactive materials. They found higher efficiency and lifetime under lower light levels for all the polymers they tested. This mainly occurs in the first and last hours of daylight, when the diffuse light is higher than direct light.

Efficiency values (Fig. 9c) at this low irradiance however show a higher variation range, as also seen in Fig. 8 for the lower  $500 \text{ W/m}^2$  data. This can be attributed to the seemingly different behaviour of the panels in diffuse only radiation and varying solar incidence angles and potentially to the sensitivity of the pyranometer at these low light levels

and to sudden irradiance changes occurring during the IV measurements, which take a few seconds to complete. However, there seem to be two different behaviour patterns seen for panel A2 and A6 efficiency values below 500 W/m²: the main trend being a sharp peak in efficiency at low irradiance of around 50–100 W/m² and then declining with increasing irradiance, the other a slower increase in efficiency with irradiance until about 500 W/m². The AM and PM data in Fig. 9 also revealed higher morning  $P_{\rm max}$ ,  $\eta$  and  $I_{\rm sc}$  values for panels A2 and A6 for the same irradiance values, indicating an overnight recovery process of the OPV panel active material. Panel A9 shows a slightly different behaviour, due to the fact that it receives its highest incident irradiance in the early morning hours, and the degradation therefore happening earlier on in the day.

To understand the effect of direct and diffuse radiation on OPVs, the sunny day 17.11.2018 and the overcast day 23.11.2018 are compared. Fig. 10 shows the percentage of diffuse irradiance from the global irradiance on these two days from the Haifa Technion meteorological station (32.7768° N, 35.0231° E) [26]. The cloudy day had a high proportion of diffuse radiation throughout the day and the radiation on the sunny day comprised of high percentage of direct radiation with a higher percentage of diffuse radiation both early morning and late afternoon.

Fig. 11 shows the diurnal behaviour of the OPV panels on those two days. For both the overcast and sunny day,  $P_{max}$  (Fig. 11b),  $I_{sc}$  (Fig. 11c)

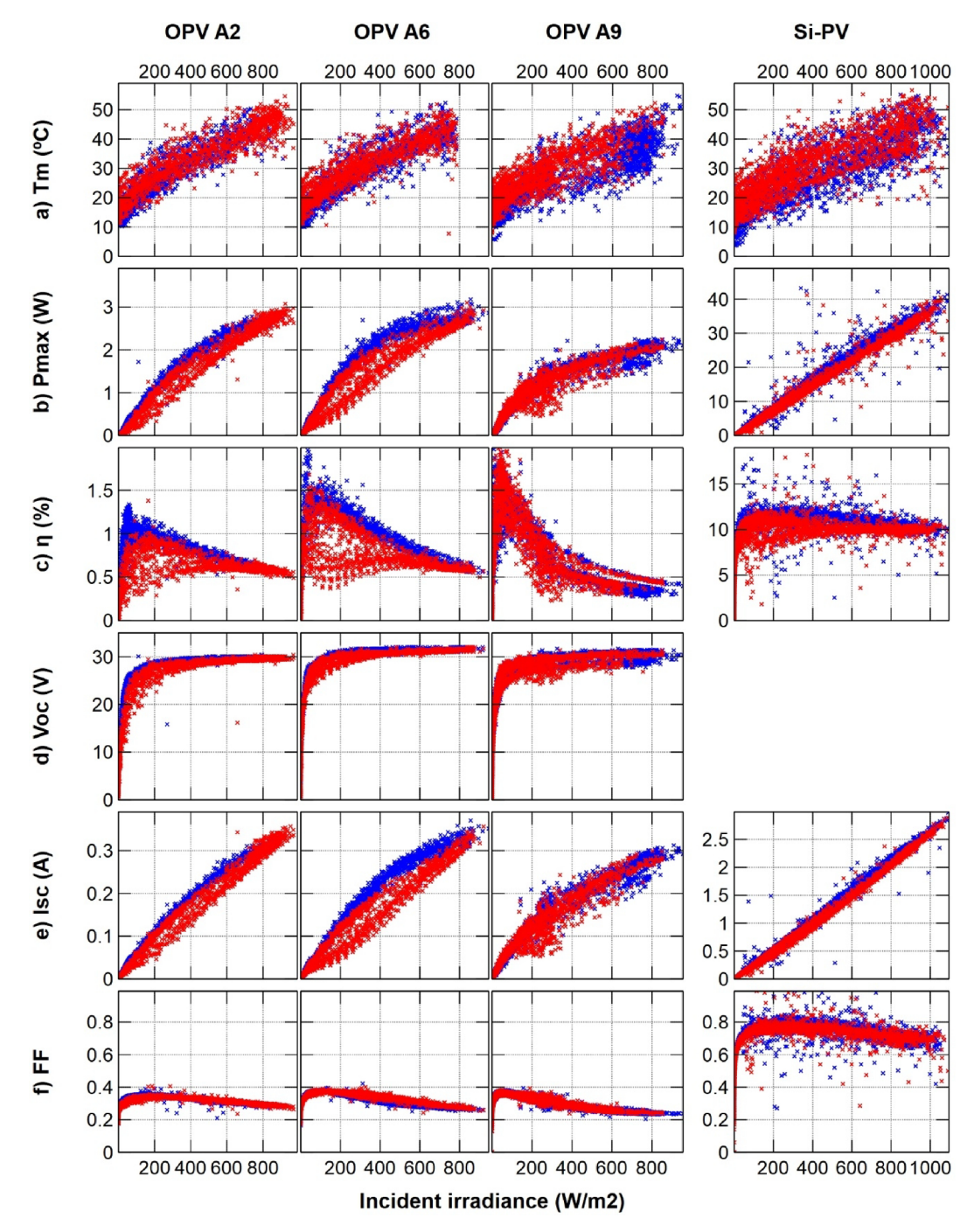


Fig. 9. Effect of irradiance on OPV and Si PV a)  $T_{ms}$ , b)  $P_{max}$ , c)  $\eta$ , d)  $V_{oc}$ , e)  $I_{sc}$  and f) FF. Blue and red symbols represent AM and PM data points respectively.

and  $T_{\rm m}$  (Fig. 11e) values followed the irradiance curves (Fig. 11a). On the overcast day, all the panels had roughly the same (mainly diffuse) incident irradiance throughout the day and therefore behaved almost the same.

On the sunny day, the Si-PV at a  $30^\circ$  tilt angle received the highest irradiance of all the panels, with its peak at midday. For the OPV panels, the incident irradiance peaked at different times as the sun moved from the Eastern side of the roof to the Western side over the course of the sunny day, providing maximum direct irradiance on panel A9 in the morning, on panel A6 at midday and on panel A2 in the afternoon. This

resulted in  $I_{sc}$ ,  $T_m$  and  $P_{max}$  values to peak at different times for each OPV panel, coinciding with their respective incident irradiance (Fig. 11a).

 $V_{\rm oc}$  values (Fig. 11d) for the OPV panels rose and remained high throughout most of the sunny day, reaching their limiting values when they received the most direct irradiance. On the overcast day,  $V_{\rm oc}$  values rose more rapidly in the morning, the limiting  $V_{\rm oc}$  values were rarely reached and more fluctuation can be seen.

On the overcast day, both efficiency and fill factor values (Graphs f and g respectively in Fig. 11) for the OPVs and Si-PV rose rapidly at

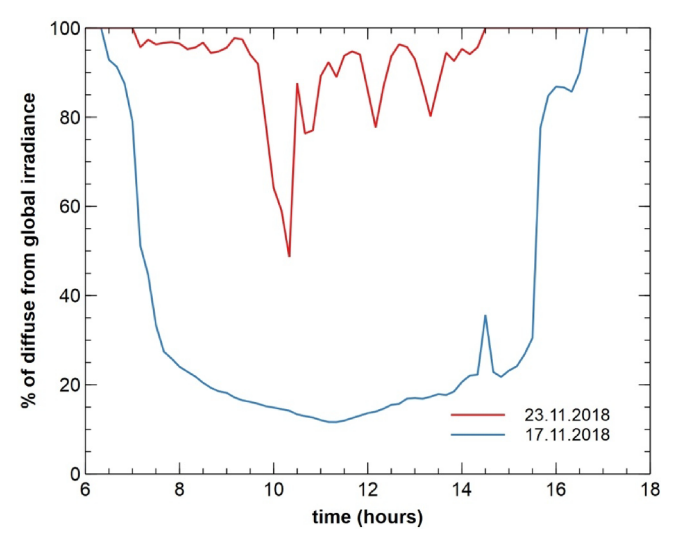


Fig. 10. Percentage of diffuse irradiance from global irradiance on the 17.11.2018 and 23.11.2018 (data for from Israel Meteorological Service [26]).

sunrise and remained at a high level throughout the day before declining at sunset. On the sunny day however, efficiency and to a lesser extent fill factor were high just after sunrise and just before sunset and dipped during the middle of the day. For the Si-PV, the dip in efficiency and fill factor at midday when the panel temperature is at its highest is explained by its negative temperature coefficient. The OPVs also behaved in a seemingly similar pattern. However, Figs. 8 and 9 showed that efficiency and fill factor were higher at times with lower irradiance, low panel temperature and more diffuse light, with their lowest values coinciding with the times of highest irradiance and panel temperature and more direct radiation, indicating these might be the influencing factors for the OPVs.

To investigate the effect of the solar incidence angle  $(\theta)$  on the performance of the panels, a smaller version of the panels was used to measure the IV curves and the incident irradiance at different solar incidence angles, as described in the Materials and Methods section above. The results for the sunny and overcast conditions of the 20.03.2019 (irradiance at measurement for  $\theta=0$ :  $1006~W/m^2)$  and the 24.03.2019 (irradiance at measurement for  $\theta=0$ :  $235~W/m^2)$  respectively are summarised in Table 2. Although  $P_{max}$  decreased as the solar incidence angle increased for both the sunny and overcast days, FF and  $\eta$  increased with larger  $\theta$  for the sunny conditions and remained relatively constant for the overcast measurements. The increase in FF and  $\eta$  with increasing  $\theta$  for the OPV panel on a sunny day concurs with other findings [31]. Overall FF and  $\eta$  were higher in the overcast conditions, as was previously described in this study.

Fig. 12 shows the diurnal variation of solar incidence angles for the 3 OPV panels at the beginning and end of the measurement period (data from [32]), showing higher angles of incidence near the end of the measurement period, due to the larger zenith angle of the sun at that time of year. Panel A6 overall had slightly higher solar incidence angles compared to A2 and A9, contributing to its higher daily average efficiency compared to panels A2 and A9 in Table 1.

### Degradation of the OPV panels

The extremely low stability of the OPVs reported by numerous other studies [13,18,20,21,30] proved to be a major hindrance to this study and the main obstacle to the feasibility of using OPVs as a greenhouse

cover. Severe degradation of the OPV panels, was recorded in this study (Figs. 13 and 14), leading to the failure of the majority of the OPV panels installed on the greenhouse roof (leaving only 3 OPVs that could be monitored). The main cause of failure was due to the movement of the roof sheeting material in windy conditions. This led to the OPVs being exposed to mechanical stresses, mainly at the panel cable connections, which lead to the degradation and electrical failure of many of the panels (Fig. 13) very early on in the study. Problems with contacts were encountered in other studies such as by Krebs et al. [18] in their round robin study. Weather, especially UV induced yellowing and brittleness of the encapsulating material and consequent delamination and degradation of the active material, as was reported by Emmott et al. [21], was also noticed in this study.

The three OPV panels that were eventually monitored in detail for this study were not the ones initially connected to the monitoring equipment and the measurement period and does therefore not include the initial operating time of the panels. For this reason, lifetime estimates or determination of  $T_{80}$  are not included in this study. Instead, it shows the operation of the panels in the more stable condition, after the initial 'burn in' period, as seen in Fig. 15.

Panel A9 showed the most degradation during the measurement period, undergoing severe and rapid degradation towards the end of the measurement period as was shown for all parameters in Fig. 15. Panels A2 and A6 did not show significant electrical degradation during the time span of the measurement period (Fig. 15). However, if assuming an initial efficiency of 3.3% at STC as specified by the manufacturers and normalising efficiency measurements at the beginning of the measurement period, the panels efficiencies had already reduced to 25–30% of their initial specified value for panels A2 and A6 and to 5–10% for panel A9, as shown in Fig. 16.

In addition to the overall non-reversible (mainly photochemical) noticed degradation, the OPV panels' performance reduced throughout the day, recovering overnight, as was described earlier. This is a phenomenon that was also noticed by Katz et al. [33] and Tromholt et al. [34] in their investigation of P3HT-PCBM and P3CT-C<sub>60</sub> cells, where they found a restoration effect of  $I_{sc}$  and  $V_{oc}$  when the cells were kept in the dark during night-time. They found that the first I<sub>sc</sub> and V<sub>oc</sub> measurements every morning yielded the highest values, which then declined during the rest of the day. They also found that shading the cells for a period of time led to a restoration effect. Isc only partly recovered and significant degradation was noticed during a month of measurements. Voc values on the other hand recovered completely every night and therefore showed almost no reduction over a longer measurement time. Katz et al. [33] proposed that this recovery phenomenon may be explained by photoinduced generation of charge traps that then slowly dissipate in the dark. Trombholt et al. [34] later investigated this reversible degradation in more detail and found that high intensity sunlight exposure brought about a major decrease in performance, which was followed by a partial recovery over time when rested in the dark or under low intensity light exposure. This process was explained as the photoactivation of the ZnO electron transport layer by O2 desorption which increased the hole conductivity, resulting in the breakdown of its diode behaviour. The recovery was explained by the re-adsorption of O2 thereby restoring the cell to near its original state.

A similar effect was also noticed in our study, although this is not a phenomenon common to all OPV device structures [18,35] where performance increased due to photo-annealing. This effect was noticed in Figs. 8 and 9, where AM  $I_{sc},\,P_{max}$  and  $\eta$  values were higher than PM values for the same irradiance values. Fig. 11 also showed high initial efficiencies in the first morning hours, which then rapidly declined and recovered to some extent late afternoon/evening and then further overnight. Panel A9 on the Eastern side of the greenhouse roof showed

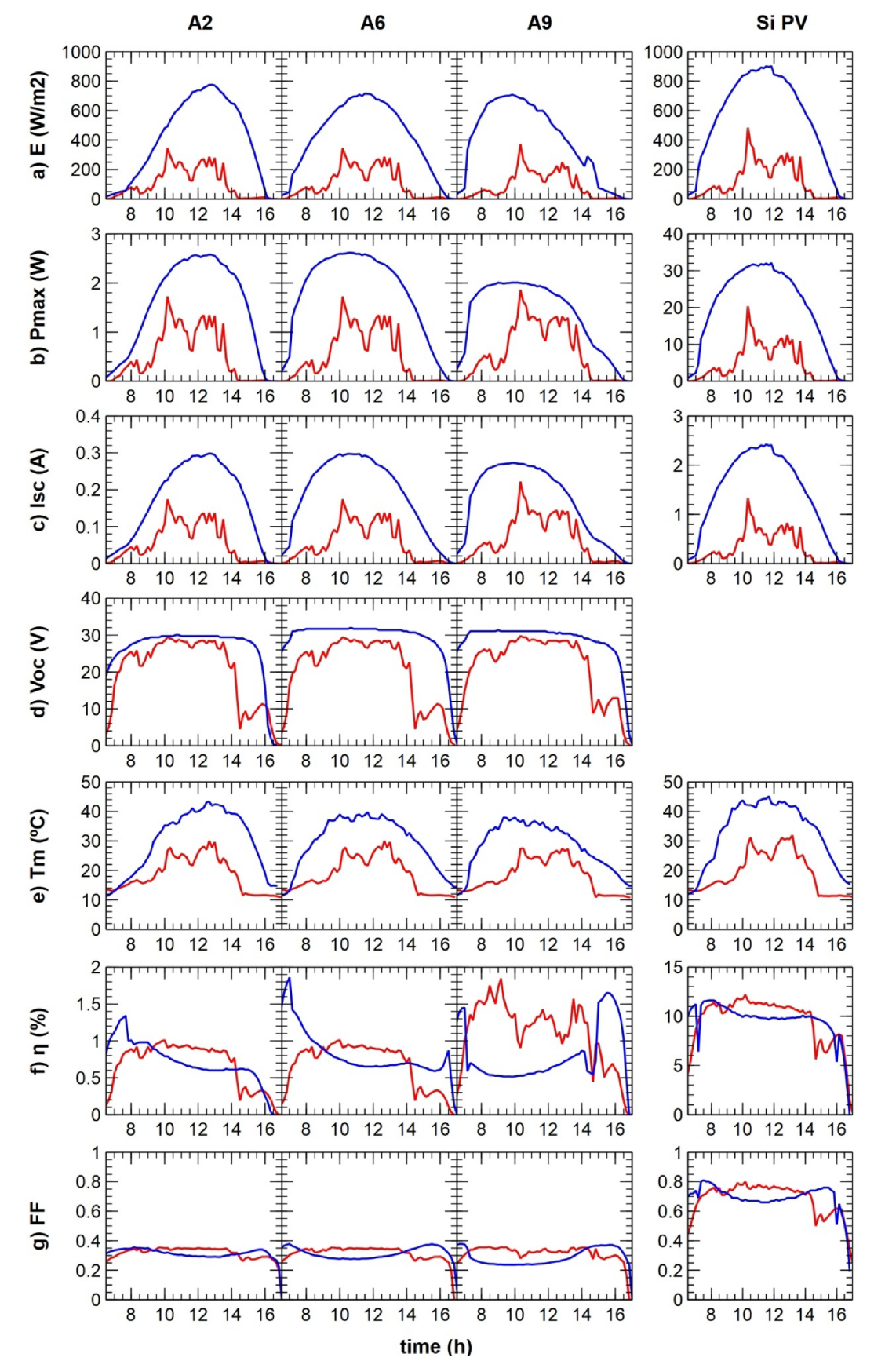
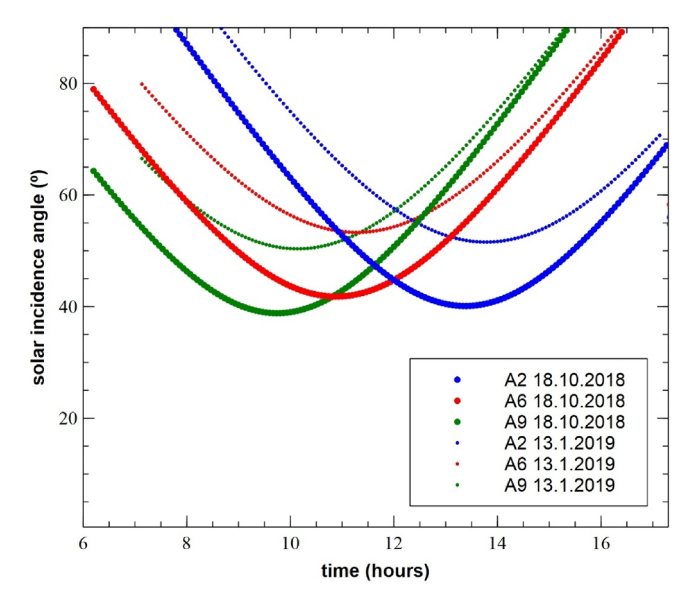


Fig. 11. a) E, b)  $P_{max}$ , c)  $I_{sc}$ , d)  $V_{oc}$ , e)  $T_m$ , f)  $\eta$  and g) FF for panels A2, A6, A9 and Si-PV on the 17.11.2018 (blue line) and 23.11.2018 (red line).

Table 2 Effect of solar incidence angle on  $P_{max},\,FF$  and  $\eta$  of an OPV panel in sunny and overcast conditions

θ	0°	10°	20°	30°	40°	50°	60°
sunny – Pmax	2.59	2.51	2.47	2.37	2.20	1.94	1.64
sunny – FF	0.37	0.39	0.38	0.40	0.40	0.42	0.44
sunny – efficiency	2.02	1.98	2.01	2.07	2.13	2.17	2.31
overcast – Pmax	0.64	0.54	0.59	0.54	0.46	0.38	0.31
overcast – FF	0.48	0.47	0.48	0.47	0.46	0.47	0.54
overcast – efficiency	2.85	2.68	2.76	2.73	2.68	2.83	2.96



**Fig. 12.** Diurnal solar incidence angles on panels A2, A6 and A9 on the first and last day of the measurement period (18.10.2018 and 13.1.2019) (data from PV Lighthouse Solar Path Calculator [32]).



Fig. 13. Degradation at the cable connection of the OPV panel.

high efficiencies for a very short time in the morning and then higher efficiencies late afternoon/evening. This was presumably due to the fact that the panel received its maximum incident irradiance earlier in the morning and therefore degraded earlier in the day and also recovered earlier than the other panels in the afternoon, when the sun moved to the Western side of the roof, leaving the Eastern side shaded.



Fig. 14. Degradation of panel active material.

#### Conclusions

This study presents a detailed analysis of the outdoor behaviour of OPV panels on a greenhouse tunnel roof, looking at, in particular, the effects of environmental variables and panel orientations on the electrical behaviour and degradation of the panels. Although other greenhouse integrated OPV studies have been carried out, this study presents the results of a detailed outdoor behaviour analysis of OPVs mounted on a polytunnel type greenhouse typical in the Mediterranean area, providing crucial outdoor testing results of greenhouse integrated OPVs in this climatic region.

In general, it was found that the OPV panel at the top of the roof yielded higher outputs, efficiencies and fill factors during the measurement period, indicating that locations on the roof with lower tilt angles would overall yield higher outputs. However, the use of panels on the East and West sides of the curved tunnel roof, could reduce midday peaks and therefore provide a more balanced power supply throughout the day, whether this is for on-site use in the greenhouse or for grid export.

The diurnal variation in OPV behaviour is influenced by simultaneous effects of changing irradiance, light spectrum and temperature. OPV outdoor behaviour results in this study, were to some extent similar to other outdoor OPV studies. At high irradiance (800 W/m<sup>2</sup>) the V<sub>oc</sub> values showed a nearly linear decrease with increasing temperature and P<sub>max</sub> and I<sub>sc</sub> appeared to slightly increase with module temperature between 40 and 55 °C. At lower irradiance (500 W/m<sup>2</sup>) that included some direct radiation,  $P_{\text{max}},\,\eta$  and  $I_{\text{sc}}$  increased with temperature. At times of mainly diffuse irradiance,  $P_{\text{max}}$ ,  $\eta$  and  $I_{\text{sc}}$  values only increased for temperatures above 35 °C. However, it was found that although output, P<sub>max</sub>, I<sub>sc</sub> and V<sub>oc</sub> values were higher with higher irradiance, the OPVs showed dips in FF and  $\eta$  at times with high direct irradiance and high temperatures despite their positive temperature coefficients. The OPV panels had higher FF and  $\eta$  at times when they received lower radiation: i.e. times with mainly diffuse irradiance or with high solar incidence angles. This was explained by a reversible degradation phenomenon in high irradiance conditions, which led to higher performance during morning hours compared to the afternoon and was followed by a recovery overnight, and to some extent in shaded conditions under lower irradiance levels. Although this phenomenon has been noticed and investigated in other device structures [33,34], this is an aspect that requires investigating further for the OPV devices used in this study to find out if this might be a common phenomenon.

The effect of the greatly varying solar incidence angles between panels in different positions on the greenhouse roof in combination

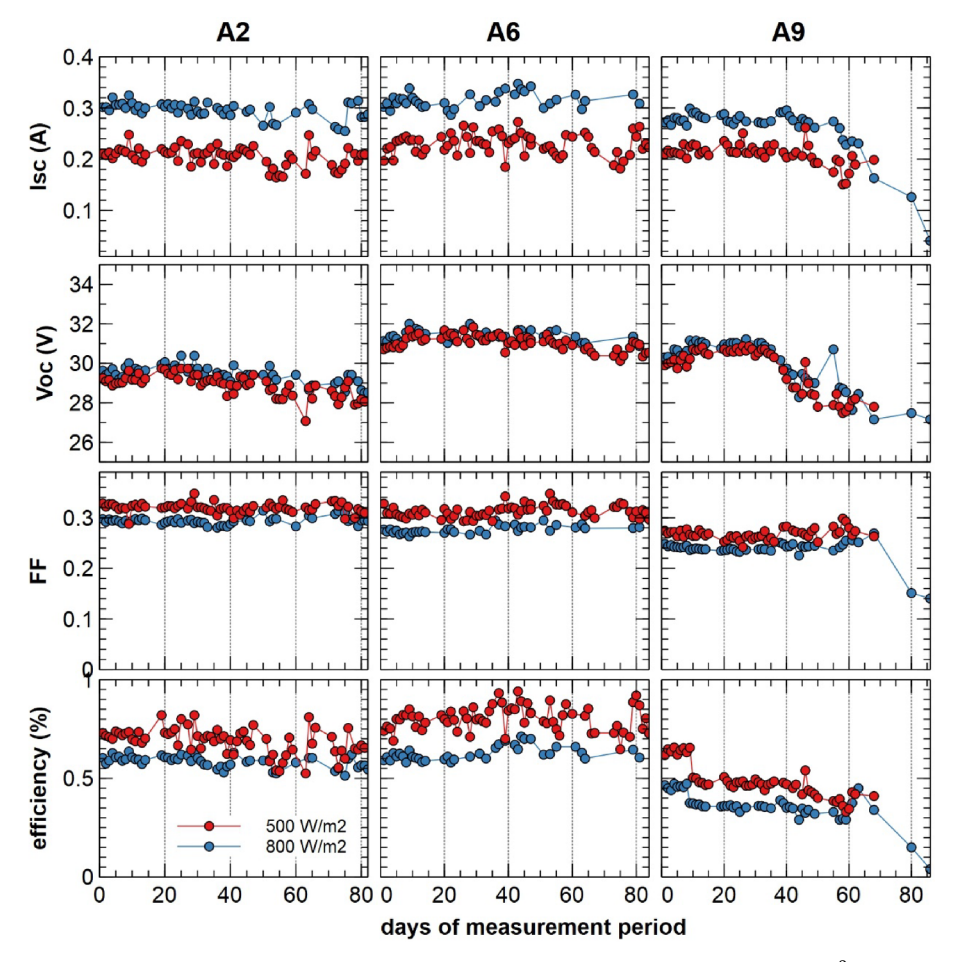


Fig. 15. Changes in  $I_{sc}$ ,  $V_{oc}$ , FF and  $\eta$  over the measurement period for incident irradiance 500  $\pm$  50 W/m $^2$  and 800  $\pm$  50 W/m $^2$ .

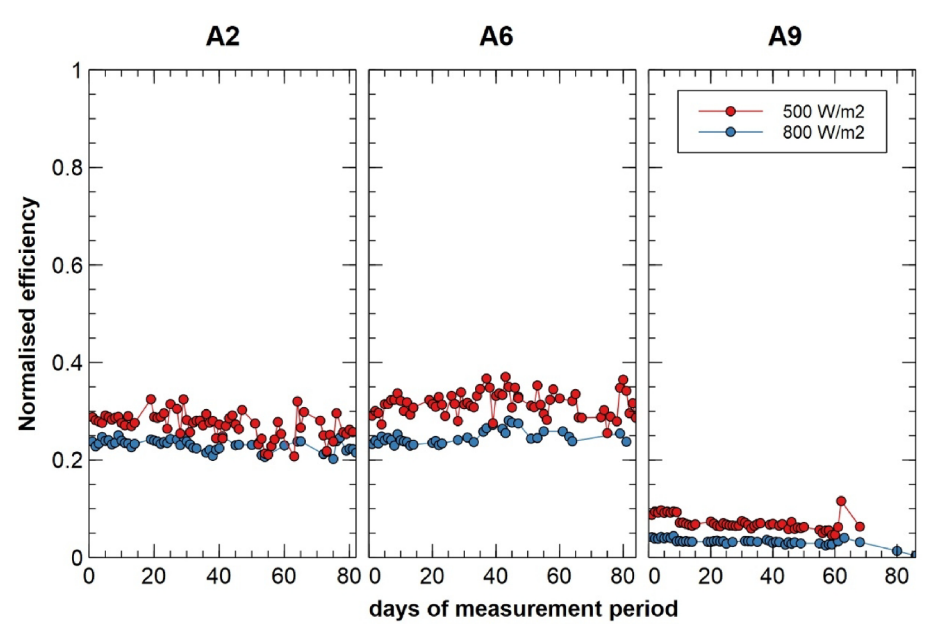


Fig. 16. Normalised efficiencies for panels A2, A6 and A9 using the same data as for Fig. 15.

with the overnight recovery aspect of the panels, would require a study with a greater number of panels in different locations on a greenhouse roof to find an optimum layout of OPVs on a greenhouse roof to achieve maximum output whilst ensuring crop quality. This more detailed study has been initiated by the authors.

The main obstacles to the feasibility of greenhouse integrated OPVs were found to be their low efficiencies and severe and rapid degradation, mainly caused by their movement, due to wind, on the greenhouse roof and exposure to high insolation (especially UV). Improved connections allowing for movement or a different mounting strategy would

need to be tested to find a better OPV panel integration method. This, coupled with the predicted improved efficiencies [36–38], could make the integration of OPVs into greenhouse covers a viable agrivoltaics solution.

### CRediT authorship contribution statement

Esther Magadley: Conceptualization, Methodology, Software, Investigation, Formal analysis, Writing - original draft. Meir Teitel: Conceptualization, Supervision, Project administration, Funding acquisition, Writing - review & editing. Maayan Friman Peretz: Writing - review & editing. Murat Kacira: Project administration, Funding acquisition, Writing - review & editing. Ibrahim Yehia: Conceptualization, Methodology, Supervision, Project administration, Funding acquisition, Writing - review & editing.

### **Declaration of Competing Interest**

The authors declare that they have no known competing financial interests or personal relationships that could have appeared to influence the work reported in this paper.

### Acknowledgements

This research was supported by Research Grant No. US-4885-16 from BARD, United States – Israel Binational Agricultural Research and Development Fund and by the Ministry of Agriculture and Rural Development of Israel (grant no. 20-12-0027).

### Appendix A. Supplementary data

Supplementary data to this article can be found online at https://doi.org/10.1016/j.seta.2020.100641.

## References

- Yano A, Cossu M. Energy sustainable greenhouse crop cultivation using photovoltaic technologies. Renewable Sustainable Energy Rev 2019;109:116–37.
- [2] Hassanien RHE, Li M, Lin WD. Advanced applications of solar energy in agricultural greenhouses. Renewable Sustainable Energy Rev 2016;54:989–1001.
- [3] Wang T, Wu G, Chen J, Cui P, Chen Z, Yan Y, et al. Integration of solar technology to modern greenhouse in China: current status, challenges and prospect. Renew Sustain Energy Rev 2017;70:1178–88.
- [4] Yano A, Furue A, Kadowaki M, Tanaka T, Hiraki E, Miyamoto M, et al. Electrical energy generated by photovoltaic modules mounted inside the roof of a north-south oriented greenhouse. Biosyst Eng 2009;103(2):228–38.
- [5] Yano A, Kadowaki M, Furue A, Tamaki N, Tanaka T, Hiraki E, et al. Shading and electrical features of a photovoltaic array mounted inside the roof of an east-west oriented greenhouse. Biosyst Eng 2010;106(4):367-77.
- [6] Campiotti C, Bibbiani C, Dondi F, Scoccianti M, Viola C. Energy efficiency and photovoltaic solar for greenhouse agriculture. J Sustainable Energy 2011;2(1).
- [7] Pérez-Alonso J, Pérez-García M, Pasamontes-Romera M, Callejón-Ferre AJ. Performance analysis and neural modelling of a greenhouse integrated photovoltaic system. Renew Sustain Energy Rev 2012;16(7):4675–85.
- [8] Cornaro C, Di Carlo A. Organic photovoltaics for energy efficiency in buildings. Nano and Biotech Based Materials for Energy Building Efficiency. Cham: Springer; 2016. p. 321–55.
- [9] Emmott CJ, Röhr JA, Campoy-Quiles M, Kirchartz T, Urbina A, Ekins-Daukes NJ, et al. Organic photovoltaic greenhouses: a unique application for semi-transparent PV? Energy Environ Sci 2015;8(4):1317–28.
- [10] Carlé JE, Helgesen M, Hagemann O, Hösel M, Heckler IM, Bundgaard E, et al. Overcoming the scaling lag for polymer solar cells. Joule 2017;1(2):274–89.
- [11] Mulligan CJ, Wilson M, Bryant G, Vaughan B, Zhou X, Belcher WJ, et al. A projection of commercial-scale organic photovoltaic module costs. Sol Energy Mater Sol Cells 2014;120:9–17.
- [12] Chatzisideris MD, Laurent A, Christoforidis GC, Krebs FC. Cost-competitiveness of organic photovoltaics for electricity self-consumption at residential buildings: a

- comparative study of Denmark and Greece under real market conditions. Appl Energy 2017;208:471–9.
- [13] Benatto GA, Corazza M, Roth B, Schütte F, Rengenstein M, Gevorgyan SA, et al. Inside or outside? Linking outdoor and indoor lifetime tests of ITO-free organic photovoltaic devices for greenhouse applications. Energy Technol 2017;5(2):338–44.
- [14] Okada K, Yehia I, Teitel M, Kacira M. Crop production and energy generation in a greenhouse integrated with semi-transparent organic photovoltaic film. In: International symposium on new technologies for environment control, energysaving and crop production in greenhouse and plant, 1227, pp. 231–240, 2017, August.
- [15] Teranaka K, Ikeda T, Doi M. Simulation of seasonal changes in radiant flux energy in a greenhouse installed with light-transmitting organic photovoltaics. In: II Asian Horticultural Congress 1208, pp. 339–346, 2016, September.
- [16] Peretz MF, Geoola F, Yehia I, Ozer S, Levi A, Magadley E, et al. Testing organic photovoltaic modules for application as greenhouse cover or shading element. Biosyst Eng 2019;184:24–36.
- [17] Hirata Y, Watanabe Y, Yachi T. Evaluation of output of transparent organic photovoltaic modules on curved surfaces depending on azimuth. In: 2018 IEEE 7th World conference on photovoltaic energy conversion (WCPEC) (A Joint Conference of 45th IEEE PVSC, 28th PVSEC & 34th EU PVSEC), pp. 1112–1115. IEEE, 2018, June.
- [18] Krebs FC, Gevorgyan SA, Gholamkhass B, Holdcroft S, Schlenker CW, Thompson ME, et al. A round robin study of flexible large-area roll-to-roll processed polymer solar cell modules. Sol Energy Mater Sol Cells 2009;93(11):1968–77.
- [19] Zhang Y, Samuel ID, Wang T, Lidzey DG. Current status of outdoor lifetime testing of organic photovoltaics. Adv Sci 2018;5(8):1800434.
- [20] Bristow N, Kettle J. Outdoor performance of organic photovoltaics: Diurnal analysis, dependence on temperature, irradiance, and degradation. J Renewable Sustainable Energy 2015;7(1):013111.
- [21] Emmott CJ, Moia D, Sandwell P, Ekins-Daukes N, Hösel M, Lukoschek L, et al. Insitu, long-term operational stability of organic photovoltaics for off-grid applications in Africa. Sol Energy Mater Sol Cells 2016;149:284–93.
- [22] Stoichkov V, Sweet TKN, Jenkins N, Kettle J. Studying the outdoor performance of organic building-integrated photovoltaics laminated to the cladding of a building prototype. Sol Energy Mater Sol Cells 2019;191:356–64.
- [23] Hartner M, Ortner A, Hiesl A, Haas R. East to west the optimal tilt angle and orientation of photovoltaic panels from an electricity system perspective. Appl Energy 2015;160:94–107.
- [24] Berny S, Blouin N, Distler A, Egelhaaf HJ, Krompiec M, Lohr A, et al. Solar trees: first large-scale demonstration of fully solution coated, semitransparent, flexible organic photovoltaic modules. Adv Sci 2016;3(5):1500342.
- [25] Reese MO, Gevorgyan SA, Jorgensen M, Bundgaard E, Kurtz SR, Ginley DS, et al. Consensus stability testing protocols for organic photovoltaic materials and devices. Sol Energy Mater Sol Cells 2011;95(5):1253–67.
- [26] Israel Meteorological Service, Irradiance database https://ims.data.gov.il/ (accessed on 12/06/2019).
- [27] Campiotti C, Viola C, Alonzo G, Bibbiani C, Giagnacovo G, Scoccianti M, et al. Sustainable greenhouse horticulture in Europe. J Sustainable Energy 2012;3(3).
- [28] Riedel I, Parisi J, Dyakonov V, Lutsen L, Vanderzande D, Hummelen JC. Effect of temperature and illumination on the electrical characteristics of polymer-fullerene bulk-heterojunction solar cells. Adv Funct Mater 2004;14(1):38–44.
- [29] Elumalai NK, Uddin A. Open circuit voltage of organic solar cells: an in-depth review. Energy Environ Sci 2016;9(2):391–410.
- [30] De Amorim Soares G, Galindo A, Chabanel M, Lima A, Vilaça R, Bagnis D. Lifetime Study on Multiple Organic Photovoltaic Materials through Outdoor Tests. VII Congresso Brasileiro de Energia Solar – Gramado, 17-20 April 2018, 2018.
- [31] Rahman MSS, Alam MK. Effect of angle of incidence on the performance of bulk heterojunction organic solar cells: a unified optoelectronic analytical framework. AIP Adv 2017;7(6):065101.
- [32] PV Lighthouse Solar Path Calculator https://www2.pvlighthouse.com.au/calculators/solar%20path%20calculator/solar%20path%20calculator.aspx (accessed on 06.04.2019).
- [33] Katz EA, Gevorgyan S, Orynbayev MS, Krebs FC. Out-door testing and long-term stability of plastic solar cells. Eur. Phys. J. Appl. Phys. 2006;36(3):307–11.
- [34] Tromholt T, Manor A, Katz EA, Krebs FC. Reversible degradation of inverted organic solar cells by concentrated sunlight. Nanotechnology 2011;22(22):225401.
- [35] Lilliedal MR, Medford AJ, Madsen MV, Norrman K, Krebs FC. The effect of post-processing treatments on inflection points in current-voltage curves of roll-to-roll processed polymer photovoltaics. Sol Energy Mater Sol Cells 2010;94(12):2018–31.
- [36] Zhao J, Li Y, Yang G, Jiang K, Lin H, Ade H, et al. Efficient organic solar cells processed from hydrocarbon solvents. Nat Energy 2016;1(2):15027.
- [37] Sun C, Pan F, Bin H, Zhang J, Xue L, Qiu B, et al. A low cost and high performance polymer donor material for polymer solar cells. Nat Commun 2018;9(1):743.
- [38] Molamohammadi S, Nia SA, Jalili YS. Improvement of inverted structure organic solar cells by Ar plasma treatment on P3HT: PC61BM active layer. Sustainable Energy Technol Assess 2019;34:43–8.